FEBS Letters 587 (2013) 2559–2564

FEBS Letters

journal homepage: www.FEBSLetters.org

The formate:oxygen oxidoreductase supercomplex of *Escherichia coli* aerobic respiratory chain

Pedro M.F. Sousa [a,b], Marco A.M. Videira [a], Ana M.P. Melo [a,*]

[a] BIOTROP, Instituto de Investigação Científica Tropical, R. da Junqueira, 86, 1°, 1300-344 Lisboa, Portugal
[b] Instituto de Tecnologia Química e Biológica, Universidade Nova de Lisboa, Av. da República (EAN), 2780-157 Oeiras, Portugal

ARTICLE INFO

Article history:
Received 10 May 2013
Revised 18 June 2013
Accepted 19 June 2013
Available online 2 July 2013

Edited by Peter Brzezinski

Keywords:
Formate:oxygen oxidoreductase activity
Aerobic respiratory chain supercomplex
Blue native polyacrylamide gel electrophoresis
Gene transcription
Bacteria
Oxygen reductase
Escherichia coli

ABSTRACT

The *Escherichia coli* formate:oxygen oxidoreductase supercomplex (FdOx) was investigated with respect to function and composition. Formate oxidoreductase activity was detected in blue native polyacrylamide gel electrophoresis (BN-PAGE) resolved membranes of *E. coli*, which were also capable of cyanide sensitive formate:oxygen oxidoreductase activity. The latter was compromised in strains devoid of specific oxygen reductases, particularly, in those devoid of cytochrome bo_3 or *bdI*. A principal component analysis (PCA) integrating *E. coli* aerobic respiratory chain gene transcription, enzyme activity and growth dynamics was performed, correlating formate:oxygen oxidoreductase activity and the transcription of the genes encoding cytochromes bo_3 and *bdI*, and corroborating previous evidence that associated these complexes in FdOx.

1. Introduction

The association of respiratory chain enzymes in supramolecular structures called supercomplexes is widespread in nature, being widely characterized in eukaryotic organisms both from the functional and structural point of view. Such organizations favor the efficiency of the oxidative phosphorylation systems, mainly due to substrate channeling and avoidance of reactive oxygen species production [1–3]. Prokaryotic respiratory chain supercomplexes have been described for a large set of microorganisms, from archaea to Gram positive and Gram negative bacteria [4–6]. In *Escherichia coli*, three supramolecular associations have been proposed: (i) the NADH oxidoreductase, (ii) the succinate:oxygen oxidoreductase and (iii) the formate:oxygen oxidoreductase (FdOx) supercomplexes (Fig. 1), according to gel based techniques and mass spectrometry evidences [7,8]. The later was unexpected since formate dehydrogenases (FDHs) and oxygen reductases were hardly related.

E. coli synthesizes three distinct membrane-associated formate dehydrogenase isoenzymes, two expressed under anaerobic conditions, FDH-H and FDH-N, and FDH-O, synthesized in the presence of oxygen or nitrate [9]. FDH-O and FDH-N are encoded by *fdoGHI* and *fdnGHI* genes. The catalytic subunits FdoG and FdnG, 110 kDa selenopolypeptides, display the highest identity and similarity, 76% and 87%, respectively, as calculated by CLUSTAL W [10] and carry out the formate-dependent reduction of dichlorophenol indophenol (DCPIP) in the presence of phenazine methosulfate (PMS) [11]. Similarly, FdoH and FdnH presented 75% identity and 85% similarity. The close relation between subunits G and H suggests that these enzymes may have similar structures.

In the present article, FdOx was investigated with respect to its function. Formate:oxygen oxidoreductase activity and the transcription of *fdoG*, the gene encoding FDH-O subunit G, was analyzed over growth. In addition, formate:oxygen oxidoreductase

Abbreviations: AU, arbitrary units; BN-PAGE, blue native polyacrylamide gel electrophoresis; DCPIP, dichlorophenol indophenol; DDM, dodecyl-β-D-maltoside; deNADH, deamino-NADH; FDH, formate dehydrogenase; FdOx, formate:oxygen oxidoreductase supercomplex; K_M, Michaelis Menten constant; MOPS, 3-(*N*-Morpholino) propanesulfonic acid; NBT, nitroblue tetrazolium; OR, oxidoreductase; PCA, principal component analysis; PMS, phenazine methosulfate; UQ_1, coenzyme Q1, analogue to ubiquinone; V_{MAX}, maximal velocity; $K_3[Fe(CN)_6]$, potassium ferricyanide; NDH-2, alternative NADH:quinone oxidoreductase; NDH-1, NADH:quinone oxidoreductase.

* Corresponding author. Address: BIOTROP, Instituto de Investigação Científica Tropical, R. da Junqueira, n° 86, 1°, 1300-344 Lisboa, Portugal. Fax: +351 213631460.

E-mail address: ana.portugal.melo@sapo.pt (A.M.P. Melo).

0014-5793/$36.00
http://dx.doi.org/10.1016/j.febslet.2013.06.031

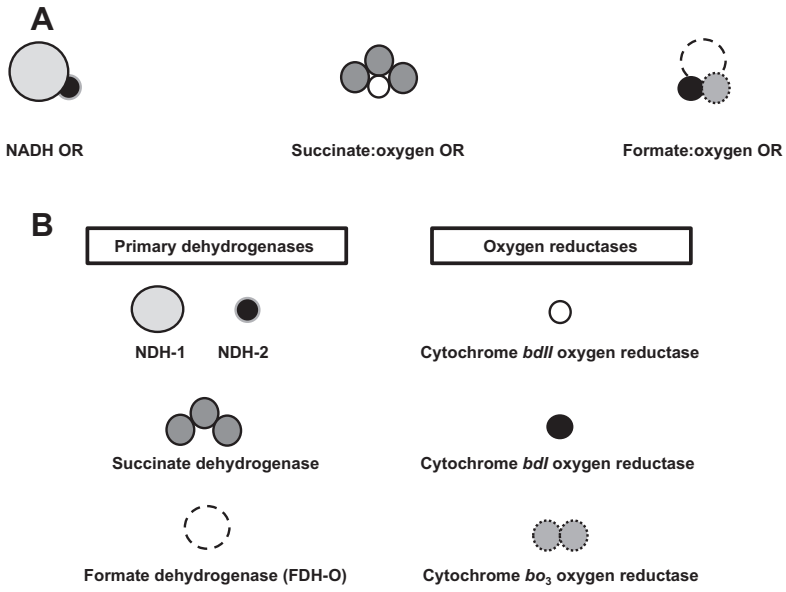

Fig. 1. Schematic representation of the *E. coli* aerobic respiratory chain supercomplexes (A) and individual complexes (B). NADH, formate:oxygen and succinate:oxygen oxidoreductase (OR) supercomplexes (A) were previously reported [7,8]. SDH [7,25] and cytochrome bo_3 oxygen reductase [7,26] are represented as trimers and dimers, respectively (B).

activity was studied in selected oxygen reductase mutants, to infer from the importance of each *E. coli* oxygen reductase in FdOx.

2. Materials and methods

2.1. Bacterial growth, cDNA synthesis and quantitative real-time PCR (qRT-PCR)

Cells from different *E. coli* strains, namely wild-type (K12), Δbo_3 (ML20S2), Δ*bdI* (ML15A), Δ*bdII* (JW0960-1) and Δ*fdoI* (JW3863) were grown aerobically and, as appropriate, harvested at mid-logarithmic (ML), early-stationary (ES), mid-stationary (MS) and late-stationary (LS) phases for RNA isolation [8] and membrane preparation [7]. The pH was monitored at harvesting steps presenting a variation of 1 pH unit and oxygen availability was ensured by growing cells under vigorous agitation in a volume corresponding to one fifth of the total volume of the flasks [8].

cDNA was synthesized and qRT-PCR experiments were performed according with [8], using oligonucleotides for *fdoG* 5′GGTGT ACGACAACCCCAATGAT and 5′GGATCAGCCATTCCAGTTTGTC.

2.2. Membrane preparation, solubilization and blue native polyacrylamide gel electrophoresis (BN-PAGE) analysis

High yields of *E. coli* inner membranes were obtained after a two-step sucrose gradient purification procedure [12], solubilized with digitonin and resolved by a 3–10% acrylamide gradient BN-PAGE. Selected lanes were further resolved in a 2D-BN-PAGE (3–10%) after incubation with 0.02% dodecyl-β-D-maltoside (DDM) and 0.05% sodium deoxycholate [13], or in harsher conditions to allow subcomplex dissociation, 0.04% DDM and 0.1% sodium deoxycholate. NADH: [7] and formate:nitroblue tetrazolium (NBT) oxidoreductase [14] artificial activities were detected *in gel*.

2.3. Enzyme activities

Enzyme activities, namely NADH:, succinate: and reduced coenzyme coenzyme Q1, analogue to ubiquinone (UQ_1) (hereon designated ubiquinol):oxygen oxidoreductase, were measured polarographicaly as previously described [8]. In addition, formate:oxygen oxidoreductase activity was also measured in a reaction buffer containing 100 mM 3-(*N*-Morpholino) propanesulfonic acid (MOPS) pH 7.2, 30 mM sodium formate and *E. coli* membranes (20 μg) from wild-type and selected respiratory chain mutant strains. The reactions were stopped by the addition of 0.5 or 2.5 mM KCN. Moreover, the same activity was tested for wild-type *E. coli* membranes harvested at different aerobic growth phases, namely ML, ES, MS and LS.

To characterize the enzyme kinetics of FDH-O, formate:oxygen oxidoreductase activity was tested using different concentrations of sodium formate (0.1–30 mM). The experiments were performed using 20 μg of *E. coli* wild-type membranes harvested at LS phase and three replicates of each assay were acquired. The Lineweaver–Burk plot [15] was obtained to determine the Michaelis Menten constant (K_M) and maximal velocity (V_{MAX}) of formate oxidation.

2.4. Principal component analysis (PCA)

Data from relative gene transcription, enzyme activity and growth dynamics were standardized and a pair-wised correlation matrix was calculated and subjected to eigenvalue decomposition to identify orthogonal components of the original matrix and generate a principal component analysis (PCA) [16] bi-plot, using the NTsys-PC (version 2.20e) software package [17]. A minimum-spanning tree was calculated in order to facilitate the visualization of the distances between operational units. Shorter distances reflect higher correlation between each component.

3. Results

3.1. Electrophoretic analysis of subcomplex composition of FdOx

To characterize FdOx, membranes from *E. coli* were resolved in a BN-PAGE and stained for NADH: (N) and formate:NBT (F) oxidoreductase activities. Bands N and F, with identical molecular masses (432 ± 7 kDa) were detected (Fig. 2). Additionally, to confirm the presence of the individual complexes in FdOx, the same procedure was applied in membranes from *E. coli* strains where FDH-O and

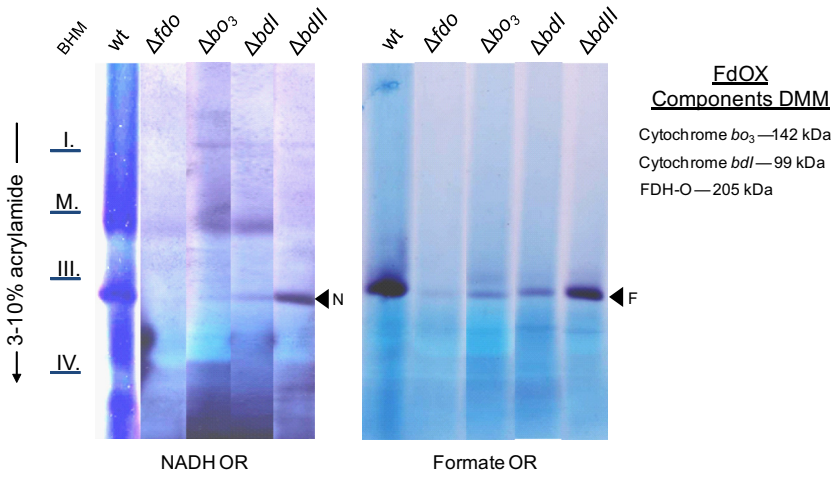

Fig. 2. *In gel* detection of the *E. coli* FdOx. Membranes from *E. coli* wild-type strain and respiratory chain mutants were resolved by BN-PAGE and the artificial oxidoreductase (OR) activities of NADH: (N) and formate:NBT (F) were detected. Digitonin solubilized bovine heart mitochondrial (BHM) complexes I, III, IV and the ATP synthase (M), were used as molecular weight markers, with 1000, 482, 205 and 597 kDa, respectively [24]. The deduced molecular masses (DMM) of FdOx individual complexes were calculated according with their amino acid sequences.

cytochromes bo_3, *bdI* and *bdII* were disrupted. Bands N and F were identified in Δ*bdII* with similar intensity to that registered for the wild-type strain, but nearly absent in the remaining mutants, thus indicating that cytochromes bo_3 and *bdI* oxygen reductases are important at least for the assembly of FdOx (Fig. 2), as previously suggested [7]. A 2D BN-PAGE was performed to investigate the dissociation of FdOx in smaller subcomplexes (Fig. 3). NADH:NBT and formate:NBT oxidoreductase activities co-localized, in bands N and F1. In addition, the formate:NBT oxidoreductase activity allowed the identification of a subcomplex of FdOx, which retained formate:NBT oxidoreductase activity, in a second smaller band, F2 (Fig. 3B).

3.2. Characterization of FdOx activity

Membranes of wild-type and selected aerobic respiratory chain mutants, namely Δbo_3, Δ*bdI*, Δ*fdo* and Δ*bdII* of *E. coli*, were investigated by means of an oxygen electrode. The rates of oxygen uptake due to NADH, succinate and ubiquinol oxidation increased in membranes where cytochromes bo_3 or *bdI* were deleted, comparatively with the wild-type (Fig. 4A–C). These activities were at least 80% inhibited by KCN, being completely inhibited when ubiquinol was used as substrate. It is noteworthy that succinate:oxygen oxidoreductase activity was severely impaired in the absence of cytochrome *bdII*, indicating the importance of this terminal oxygen reductase when succinate is oxidized, in agreement with the proposed supercomplex composed by SDH and cytochrome *bdII* [8]. In contrast, formate:oxygen oxidoreductase activity was higher in membranes from wild-type and cytochrome *bdII* mutant strains (Fig. 4D), displaying a KCN inhibition of 90%, and was barely detectable in Δbo_3, Δ*bdI* and Δ*fdo* membranes, corroborating evidences from BN-PAGE (Fig. 2) and mass spectrometry results [7]. This is the first time that cyanide sensitive formate:oxygen oxidoreductase activity was detected in *E. coli* membranes.

FdOx activity was monitored during wild-type *E. coli* aerobic growth at ML, ES, MS and LS phases. Formate:oxygen oxidoreductase activity was maximal at ML and ES growth stages, decreased about 20% at MS and dropped to nearly 25% at LS. 90% of KCN inhibition was displayed in all growth stages (Fig. 5A).

The kinetics of FdOx was investigated in *E. coli* membranes establishing the apparent K_M and V_{MAX} of formate oxidation, at pH 7.2, by measuring the rate of formate oxidation in response to a range of formate concentrations. Lineweaver–Burk plots were generated and the kinetic parameters calculated according with [15] (SM1). The K_M of formate oxidation was 169 ± 21 μM and

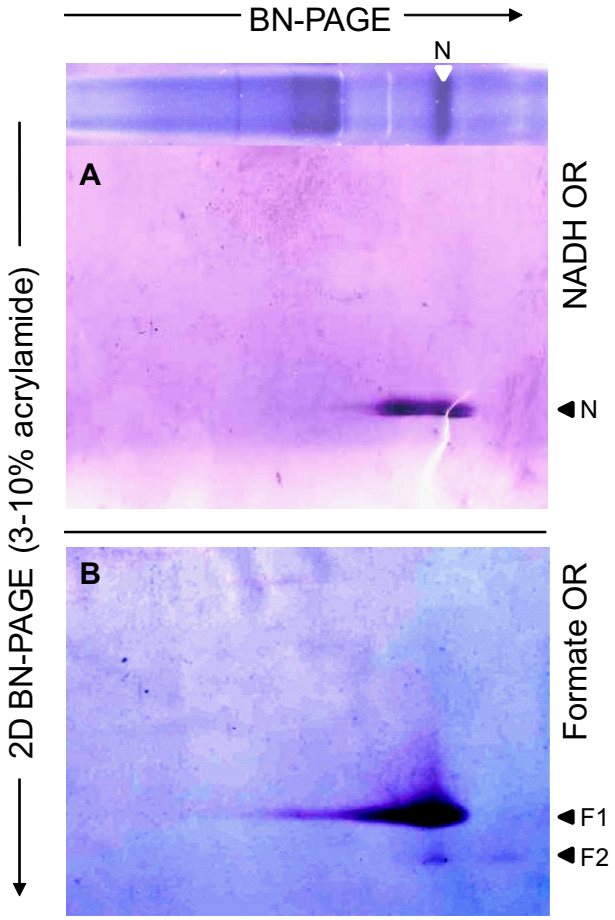

Fig. 3. Identification of FdOx supercomplex by 2D BN-PAGE. Lanes derived from the first dimension BN-PAGE were resolved in a second dimension BN-PAGE and detected for NADH: (A) and formate:NBT oxidoreductase (B) activities, retrieving bands N and F1 corresponding to FdOx, and a smaller subcomplex with formate:NBT oxidoreductase activity, F2.

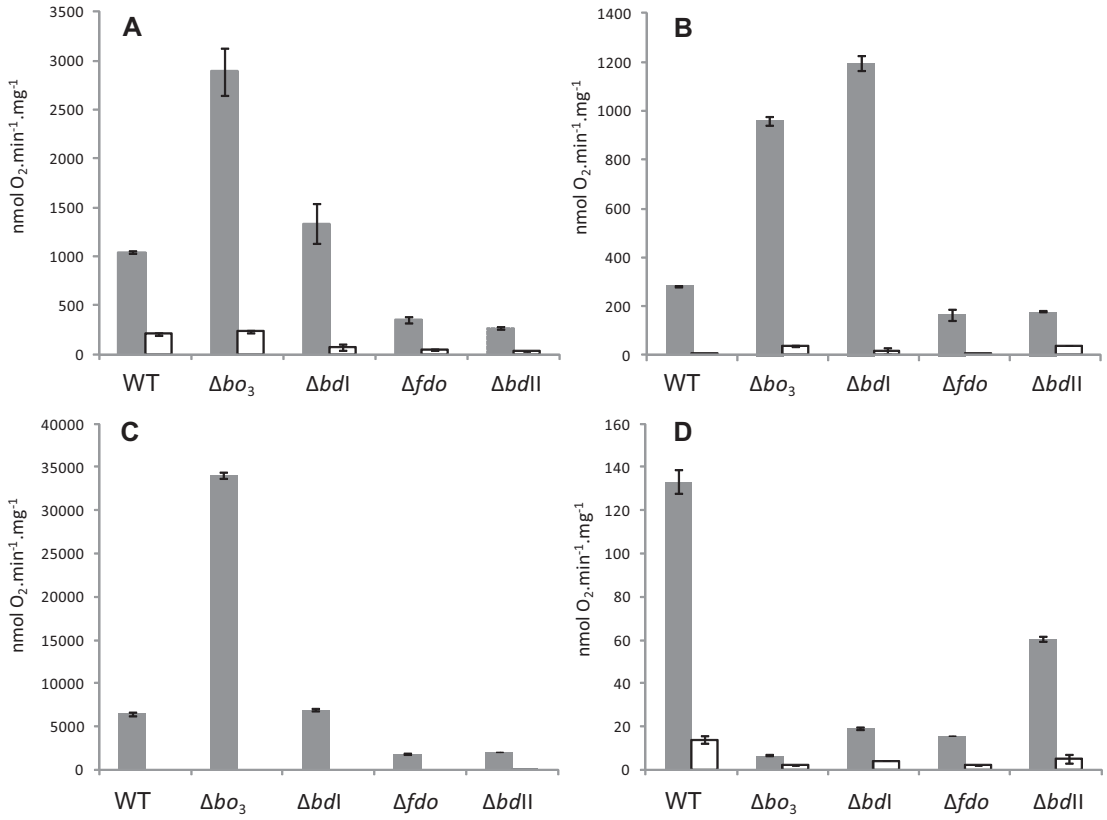

Fig. 4. Oxidation rate of respiratory chain substrates in *E. coli* membranes of wild-type, Δ*bo*$_3$, Δ*bdI*, Δ*fdo* and Δ*bdII* strains. Oxygen consumption was measured upon NADH (A), succinate (B), ubiquinol (UQ_1) (C) and formate addition (D) (nmol O_2 min^{-1} mg^{-1}) on *E. coli* (grey bars). The addition of KCN inhibited oxygen consumption by at least 80%, this inhibition being complete when UQ1 was used as substrate. 90% of formate:oxygen oxidoreductase inhibition by KCN was displayed in both wild-type and Δ*bdII*.

the corresponding V_{MAX} 117 ± 15 nmol O_2 min^{-1} mg^{-1}. The K_M value is of the same order of magnitude of FDH-N K_M (120 μM) [11] being reasonable to assume that it may play the same physiological role of the anaerobic counterpart at neutral pH, suggested to oxidize the formate excreted from the cytoplasm and compartmentalized in the periplasm [18].

3.3. Integrative analysis of FdOx: bacterial growth, enzyme activity and gene transcription

In order to evaluate the prevalence of FDH-O along the *E. coli* aerobic growth and to compare the variation of *fdoG* transcription profile with that of other *E. coli* aerobic respiratory chain genes [8], the relative transcription of *fdoG* was analyzed by qRT-PCR at ML, ES, MS and LS growth stages. *fdoG* transcription levels were maximal at ML, dropping to 25% at ES, increasing to 50% at MS and dropping again to 33% at LS growth stage (Fig. 5B), similarly to *ndh* relative transcription profile [8]. Interestingly, the growth stage where *fdoG* relative transcription values were lowest, ES, presented the highest values of oxygen consumption due to formate oxidation in *E. coli* wild-type membranes (Fig. 5A). Such variation is in agreement with what is observed when comparing the relative transcription of *nuoF* and *ndh* genes with the oxygen consumption profile over growth due to NADH oxidation [8].

A PCA bi-plot was acquired from the activity and transcription data of FdOx and *fdoG* and the dataset obtained in [8] (Fig. 6). *fdoG* relative transcription and FdOx activity were negatively correlated with the growth progress (OD_{600}), as deduced by their relative position in the PCA bi-plot. Moreover, the activity profile of FdOx along growth is not correlated with the other oxygen oxidoreductase activities, namely succinate:, ubiquinol: and NADH:oxygen oxidoreductase activities (see [8]). Finally, according to the PCA and supported by the minimum-length spanning tree and apart from the strong positive correlation confirmed between *ndh* and *nuoF* [8], the nearest variables connecting *fdoG* gene were *cydA*, formate:oxygen oxidoreductase activity and *cyoB*, in agreement with the composition and enzymatic activity of the supercomplex herein characterized.

4. Discussion

This work provided evidences to support the existence of a functional FdOx supercomplex with cyanide sensitive formate:oxygen oxidoreductase activity in the aerobic respiratory chain of *E. coli*. BN-PAGE (Figs. 2 and 3) analysis and the positive correlation established between the formate:O_2 oxidoreductase activity and the transcription of *cyoB* and *cydA* genes, which encode subunits of *bo*$_3$ and *bdI* oxygen reductases (Fig. 6), respectively, confirmed that FdOx supercomplex is composed by these three complexes. In addition, it was demonstrated that *bo*$_3$ and *bdI* oxygen reductases are crucial for FdOx activity (Fig. 4D).

A supramolecular structure like FdOx may contribute to the generation of a proton motive force from the oxidation of formate, with energy conservation, since *bo*$_3$ and *bdI* oxygen reductases are electrogenic [19]. In fact, cytochrome *bo*$_3$ is the only proton-pumping oxygen reductase present in the *E. coli* respiratory chain [20].

Previous reports suggested that FDH-O is synthesized in the presence of oxygen [9] and able of formate oxidation in whole cells when oxygen is present [9,21], very likely via FdOx, at the light of the findings presented herein. Formate is a highly reducing compound ($E_{m,7}$ −420 mV) and under aerobic conditions FDH-O is the best candidate to prevent formate accumulation in cells.

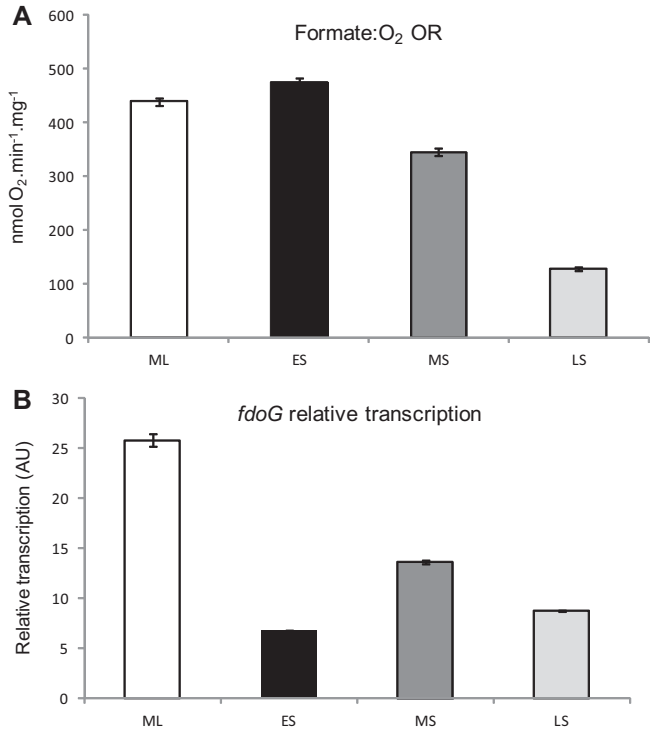

Fig. 5. Formate:oxygen oxidoreductase activity (A) and *fdoG* relative transcription (B) during aerobic growth. *E. coli* wild-type membranes were harvested at mid-logarithmic (white), early-stationary (black), mid-stationary (dark-grey) and late-stationary (light-grey) growth phases. Relative transcription levels of *fdoG* along the aerobic growth were analyzed together with the dataset reported for other *E. coli* aerobic respiratory chain components [8]. The transcription of *fdoG* at each curve point was normalized to the 16S rRNA reference gene and calculated in function of the most expressed gene/condition of the whole dataset, ML-*nuoF* [8]. (For interpretation of the references to colour in this figure legend, the reader is referred to the web version of this article.)

Furthermore, the assembly of the aerobic formate dehydrogenase and bo_3 and *bdI* oxygen reductases in a functional supercomplex is in agreement with older evidences that suggest ubiquinone, rather than menaquinone, to be the electron acceptor of formate oxidation [22].

As previously mentioned, the catalytic subunit G of FDH-N is highly similar to that of FDH-O, thus being reasonable to expect that the FDH-O active site faces the periplasmic side of the cytoplasmic membrane as it was proposed in the structure of FDH-N [23].

Acknowledgments

The authors would like to thank Dr. Robert Gennis for the generous gift of the *E. coli* mutant strains ML20S2 and ML15A, and *E. coli* Genetic Stock Center for supplying *E. coli* JW0960-1 and JW3863 strains. Dr. Luis Goulao is acknowledged for helpful discussions regarding the PCA analysis and the statistic results. Micaela Sousa, Elisabete Lopes and Isabel Palos are acknowledged for excellent technical assistance. P.S. is a recipient of the FCT Grant SFRH/BD/46553/2008.

Appendix A. Supplementary data

Supplementary data associated with this article can be found, in the online version, at http://dx.doi.org/10.1016/j.febslet.2013.06.031.

References

[1] Lenaz, G. and Genova, M.L. (2009) Mobility and function of coenzyme Q (ubiquinone) in the mitochondrial respiratory chain. Biochim. Biophys. Acta 1787, 563–573.
[2] Diaz, F., Enríquez, J.A. and Moraes, C.T. (2012) Cells lacking Rieske iron–sulfur protein have a reactive oxygen species-associated decrease in respiratory complexes I and IV. Mol. Cell. Biol. 32, 415–429.
[3] Lenaz, G. and Genova, M.L. (2012) Supramolecular organisation of the mitochondrial respiratory chain: a new challenge for the mechanism and control of oxidative phosphorylation. Adv. Exp. Med. Biol. 748, 107–144.
[4] Iwasaki, T., Matsuura, K. and Oshima, T. (1995) Resolution of the aerobic respiratory system of the thermoacidophilic archaeon, *Sulfolobus sp.* strain 7. I. The archaeal terminal oxidase supercomplex is a functional fusion of respiratory complexes III and IV with no *c*-type cytochromes. J. Biol. Chem. 270, 30881–30892.
[5] Sone, N., Sekimachi, M. and Kutoh, E. (1987) Identification and properties of a quinol oxidase super-complex composed of a bc_1 complex and cytochrome oxidase in the thermophilic bacterium PS3. J. Biol. Chem. 262, 15386–15391.
[6] Berry, E.A. and Trumpower, B.L. (1985) Isolation of ubiquinol oxidase from *Paracoccus denitrificans* and resolution into cytochrome bc_1 and cytochrome *c*-aa_3 complexes. J. Biol. Chem. 260, 2458–2467.
[7] Sousa, P.M.F., Silva, S.T.N., Hood, B.L., Charro, N., Carita, J.N., Vaz, F., Penque, D., Conrads, T.P. and Melo, A.M.P. (2011) Supramolecular organizations in the aerobic respiratory chain of *Escherichia coli*. Biochimie 93, 418–425.
[8] Sousa, P.M.F., Videira, M.A.M., Bohn, A., Hood, B.L., Conrads, T.P., Goulao, L.F. and Melo, A.M.P. (2012) The aerobic respiratory chain of *Escherichia coli*: from genes to supercomplexes. Microbiology 158, 2408–2418.
[9] Sawers, G., Heider, J., Zehelein, E. and Böck, A. (1991) Expression and operon structure of the sel genes of *Escherichia coli* and identification of a third

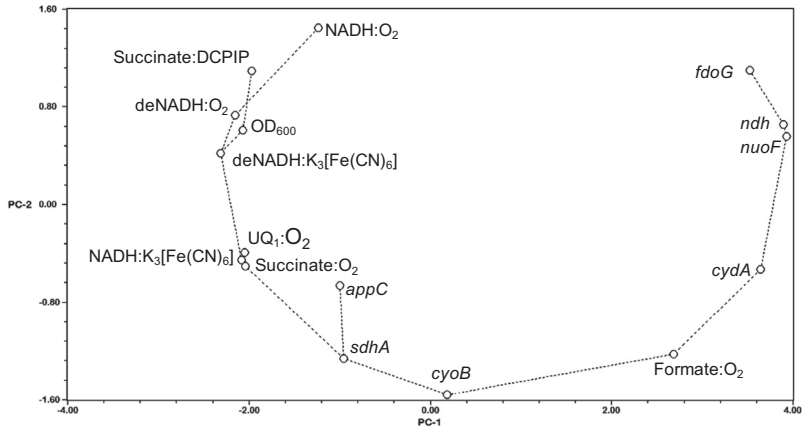

Fig. 6. PCA applied to relative gene transcription, oxidoreductase activity and growth dynamics values of *E. coli* aerobic respiratory chain. The first two principal components account for 92.8% of the total variation, from which PC-1 and PC-2 correspond to 67.9% and 24.9% of variance, respectively. A minimum-length spanning tree connecting the nearest variables based on the correlation matrix is superimposed.

selenium-containing formate dehydrogenase isoenzyme. J. Bacteriol. 173, 4983–4993.
[10] Thompson, J.D., Higgins, D.G. and Gibson, T.J. (1994) CLUSTAL W: improving the sensitivity of progressive multiple sequence alignment through sequence weighting, position-specific gap penalties and weight matrix choice. Nucleic Acids Res. 22, 4673–4680.
[11] Sawers, G. (1994) The hydrogenases and formate dehydrogenases of *Escherichia coli*. Antonie Van Leeuwenhoek 66, 57–88.
[12] Stenberg, F., Chovanec, P., Maslen, S.L., Robinson, C.V., Ilag, L.L., von Heijne, G. and Daley, D.O. (2005) Protein complexes of the *Escherichia coli* cell envelope. J. Biol. Chem. 280, 34409–34419.
[13] Wittig, I., Braun, H.P. and Schägger, H. (2006) Blue native PAGE. Nat. Protoc. 1, 418–428.
[14] Enoch, H.G. and Lester, R.L. (1975) The purification and properties of formate dehydrogenase and nitrate reductase from *Escherichia coli*. J. Biol. Chem. 250, 6693–6705.
[15] Lineweaver, H. and Burk, D. (1934) The determination of enzyme dissociation constants. J. Am. Chem. Soc. 56, 658–666.
[16] Jolliffe, I.T. (2002) Principal Component Analysis, Springer, New York, USA.
[17] Rohlf, F.J. (2005) NTSYS-pc, Numerical Taxonomy and Multivariate Analysis Systemed, Exeter Software, Setauket, New York, USA.
[18] Sawers, R.G. (2005) Formate and its role in hydrogen production in *Escherichia coli*. Biochem. Soc. Trans. 33, 42–46.
[19] Puustinen, A., Finel, M., Haltia, T., Gennis, R.B. and Wikström, M. (1991) Properties of the two terminal oxidases of *Escherichia coli*. Biochemistry 30, 3936–3942.
[20] Puustinen, A., Finel, M., Virkki, M. and Wikström, M. (1989) Cytochrome *o* (*bo*) is a proton pump in *Paracoccus denitrificans* and *Escherichia coli*. FEBS Lett. 249, 163–167.
[21] Pinsent, J. (1954) The need for selenite and molybdate in the formation of formic dehydrogenase by members of the coli-aerogenes group of bacteria. Biochem. J. 57, 10–16.
[22] Giordano, G., Grillet, L., Rosset, R., Dou, J.H., Azoulay, E. and Haddock, B.A. (1978) Characterization of an *Escherichia coli* K12 mutant that is sensitive to chlorate when grown aerobically. Biochem. J. 176, 553–561.
[23] Jormakka, M., Törnroth, S., Byrne, B. and Iwata, S. (2002) Molecular basis of proton motive force generation: structure of formate dehydrogenase-*N*. Science 295, 1863–1868.
[24] Wittig, I., Beckhaus, T., Wumaier, Z., Karas, M. and Schägger, H. (2010) Mass estimation of native proteins by blue native electrophoresis: principles and practical hints. Mol. Cell. Proteomics 9, 2149–2161.
[25] Yankovskaya, V. et al. (2003) Architecture of succinate dehydrogenase and reactive oxygen species generation. Science 299, 700–704.
[26] Stenberg, F., von Heijne, G. and Daley, D.O. (2007) Assembly of the cytochrome bo_3 complex. J. Mol. Biol. 371, 765–773.